A 3D VISUAL SERVOING SYSTEM

Mircea Ivănescu*, Dorian Cojocaru*,
Nirvana Popescu, Decebal Popescu**,**
Răzvan Tudor Tănasie***

**University of Craiova, Mechatronics Department,*
***University Politehnica of Bucharest, Computers Department,*
****University of Craiova, Software Engineering Department*

Abstract - The control problem of a hyperredundant manipulator by using a robust 3 D visual servoing is presented. The theoretical model of this class of arms is studied. Servoing is based on binocular vision obtained by two cameras that ensure a continuous measure of the arm parameters. The control errors function is built in 3D cartesian space by the visual information obtained in the two image planes. The 2D errors are determined as the shape errors, they are calculated on the differences between the actual and desired continuous angle values. A spatial error is determined and a control law is discussed. The stability of the closed-loop control system is proven. Computer simulations are presented to show the applicability of the method.

Keywords: hyperredundant manipulator, visual servoing, distributed parameter system.

1. INTRODUCTION

An ideal hyperredundant manipulator is a non-conventional robotic arm with an infinite mobility. It has the capability to take sophisticated shapes and to achieve any position and orientation in a 3D space. These systems are also known as Hyper-Degree-Of-Freedom (HDOF) manipulators and, over the past several years, there has been a rapidly expanding interest in the study and construction of them.

The control of these systems is very complicated and a great number of researchers tried to offer solutions for this difficult problem. In (Hemami, 1984) it was analysed the control by cables or tendons meant to transmit forces to the elements of the arm in order to closely approximate the arm as a truly continuous backbone. Also, Mochiyama has investigated the problem of controlling the shape of an HDOF rigid-link robot with two-degree-of-freedom joints using spatial curves (Mochiyama and Kobayashi, 1999; Robinson and Davies, 1999). Important results were obtained by Chirikjian and Burdick that laid the foundations for the kinematic theory of hyperredundant robots. Their results are based on a "backbone curve" that captures the robot's macroscopic geometric features. The inverse kinematic problem is reduced to determining the time varying backbone curve behaviour. New methods for determining "optimal" hyper-redundant manipulator configurations based on a continuous formulation of kinematics are developed. In (Gravagne and Walker, 2000), Gravagne analysed the kinematic model of "hyper-redundant" robots, known as "continuum" robots. Robinson and Davies (Robinson and Davies, 1999) present the "state of art" of continuum robots, outline their areas of application and introduce some control issues. The great number of parameters, theoretically an infinite number, makes very difficult the use of classical control methods and the conventional transducers for position and orientation.

In this paper the method of image-based servoing (Hutchinson et al., 1996; Adachi and Sato, 2004) for a hyperredundant arm is studied. Servoing is based on binocular vision, a continuous measure of the arm parameters derrived from the real-time computation of the binocular optical flow over the two images, is

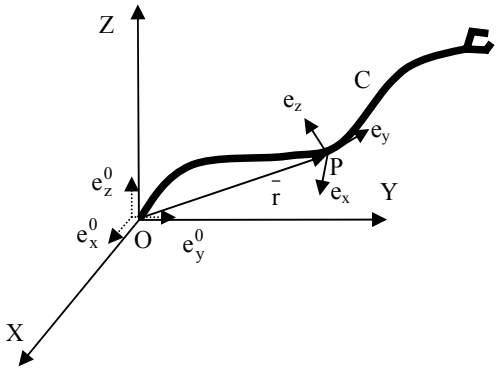

Fig. 1.

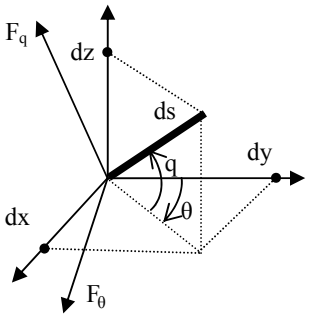

Fig. 2.

compared with the desired position of the arm. The control error function is built in 3D cartesian space by the visual information obtained by two cameras in two image planes (Grosso et al., 1996). The two 2D errors obtained in the two image planes are determined by the two differences between the actual and desired continuous angle values that define the projections of the arm shape. The plane errors can be considered as the errors of the arm shape. These errors are used to calculate the spatial error and a control law is synthesized. For the closed-loop control system and a control law the stability is proven by using the Lyapunov second method. The error function is computed in the image spaces virtually and no calibration (camera parameters) is required allowing the synthesis of more robust control laws.

The paper is organised as follows: Section 2 reviews the basic principles of a hyperredundant manipulator; Section 3 presents the camera video system; Section 4 introduces the servoing system; Section 5 verifies by computer simulations the control law.

2. BACKGROUND

Consider a 3D hyperredundant robot with a three dimensional Cartesian coordinate frame called the robot coordinate frame whose axes are labeled X, Y, Z. The mechanical structure represents an ideal arm, with an uniform distributed mass and torque, with ideal flexibility that can take any arbitrary shape (Fig. 1). We will neglect friction and structure damping. The essence of the model is a 3 – dimensional backbone curve C that is parametrically described by a vector $r(s) \in \Re^3$ and an associate frame $\Phi(s) \in \Re^3$ whose columns create the frame base (Fig. 2) (Gravagne and Walker, 2000; Chirikjian and Burdick, 1990). The independent parameter s is related to the arc length from the origin of the curve C. The position of a point s on the curve C is defined by the position vector,

$$\bar{r} = \bar{r}(s) \qquad (2.1)$$

where $s \in [0,l]$. For a dynamic motion, the time variable is introduced, $\bar{r} = \bar{r}(s,t)$.

The parametrisation of the curve C is based upon two "continous angle" $\theta(s)$ and q(s) (Chirikjian and Burdick, 1990; Chirikjian, 1993) (Fig. 2). At each point $\bar{r}(s,t)$, the robot's orientation is given by a right-handed orthonormal basis vector $\{\bar{e}_x, \bar{e}_y, \bar{e}_z\}$ and its origin coincides with the point $\bar{r}(s,t)$. The set of backbone frames can be parametrized as

$$\Phi^s(t) = \left(\bar{e}_x(s,t), \bar{e}_y(s,t), \bar{e}_z(s,t)\right) \qquad (2.2)$$

The pointer vector on curve C is given by

$$\bar{r}(s,t) = \left(x(s,t), y(s,t), z(s,t)\right)^T \qquad (2,3)$$

where

$$x(s,t) = \int_0^s \sin\theta(s',t)\cdot\cos q(s',t)\cdot ds'$$

$$y(s,t) = \int_0^s \cos\theta(s',t)\cdot\cos q(s',t)\cdot ds' \qquad (2.4)$$

$$z(s,t) = \int_0^s \sin q(s',t)\cdot ds'$$

where $s' \in [0,s]$.

We adopt the following interpretation (Chirikjian and Burdick, 1995; Mochiyama and Kobayashi, 1999): at any point s the relation (2.4) determines the current position and Φ^s determines the robot's orientation and the robot's shape is defined by the behaviour of function θ(s) and q(s). The robot "grows" from the origin by integrating to get $\bar{r}(s,t)$, $s \in [0,l]$. By using this definition, two position of the hyperredundant can be defined by a curve C as

$$C : (\theta(s), q(s)) \quad , s \in [0,l] \qquad (2,5)$$

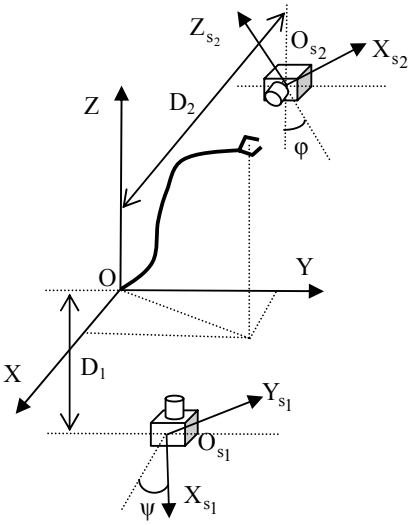

Fig. 3.

The motion and orientation of the arm are given by the distributed forces on the legth of the arm, $F_\theta(s,t)$ and $F_q(s,t)$ that rotate the element ds in the planes of the angles θ(s) and q(s), respectively. The manipulator model is considered as a distributed parameter system defined on a fixed spatial domain [0,l] and the spatial coordinate is s.

The dynamic model of this manipulator with hyperredundant configuration can be obtained from Hamilton partial differential equations (Wang, 1965).

$$\frac{\partial\omega(t,s)}{\partial t} = \frac{\delta H}{\delta\nu(t,s)} \qquad (2.6)$$

$$\frac{\partial\nu(t,s)}{\partial t} = -\frac{\delta H}{\delta\omega(t,s)} + F(t,s)$$

where ω and ν are the generalised coordinates and momentum derivated respectively and $\delta(.)/\delta(.)$ denotes a functional partial derivative.

The state of the system ot any fixed time t is specified by the set $(\omega(t,s),\nu(t,s))$, where $\omega \in [\theta \quad q]^T$ The control force is a distributed force along the arm

$$F = \begin{bmatrix} F_\theta & F_q \end{bmatrix}^T \qquad (2.7)$$

3. CAMERA SYSTEM

Two video cameras provide two images of the whole robot workspace. The two images planes are parallel with XOY and ZOY planes from robot coordinate frame, respectively (Fig. 3). The cameras provide the images of the scene that stored in the frame grabber's video memory being displayed on the computer screens. Related to the image planes are defined two dimensional coordinate frames, called screen coordinate frames or image coordinate systems. Denote X_{S_1}, Y_{S_1} and Z_{S_2}, Y_{S_2} respectively, the axes of the two screen coordinate frames provided by the two cameras. The spatial centers for each camera are located at the distances D_1 and D_2, with respect to the XOY and ZOY planes, respectively. The orientation of the cameras arround the optical axes with respect to the robot coordinate frame, are noted by ψ and φ , respectively. A point P in the coordinate frame is

$$P=[\,x,\,y,\,z]^T \qquad (3.1)$$

The description of a point P in the two screen coordinate frames are denoted by

$$P_{S_1} = [\,x_{S_1},\, y_{S_1}\,] \qquad (3.2)$$

$$P_{S2} = [\,z_{S_2},\, y_{S_2}\,] \qquad (3.3)$$

Geometric optics are used to model the mapping between the robot Cartesian space and the screen coordinate systems. We assume that the quantization and the lens distortion effects are negligible. The description of the point P=[x, y, z]T in the robot coordinate frame is given in terms of screen coordinate frames as (Kelly, 1996)

$$\begin{bmatrix} x_{s_1} \\ y_{s_1} \end{bmatrix} = \alpha_1 \cdot \frac{\lambda_1}{\lambda_1 - (D_1 + x)} \cdot R(\varphi) \cdot \cdot \left\{ \begin{bmatrix} x \\ y \end{bmatrix} - \begin{bmatrix} o_{11} \\ o_{12} \end{bmatrix} \right\} + \begin{bmatrix} c_{x_1} \\ c_{y_1} \end{bmatrix} \qquad (3.4)$$

for the $Z_{S_1} O_{S_1} Y_{S_1}$ frame and

$$\begin{bmatrix} z_{s_2} \\ y_{s_2} \end{bmatrix} = \alpha_2 \cdot \frac{\lambda_2}{\lambda_2 - (D_2 + x)} \cdot R(\varphi) \cdot \cdot \left\{ \begin{bmatrix} z \\ y \end{bmatrix} - \begin{bmatrix} o_{21} \\ o_{22} \end{bmatrix} \right\} + \begin{bmatrix} c_{z_2} \\ c_{y2} \end{bmatrix} \qquad (3.5)$$

for the $Z_{S_2} O_{S_2} Y_{S_2}$ frame, where $[\,c_{x_1}, c_{y_1}\,]^T$ and $[\,c_{z_2}, c_{y_2}\,]^T$ the image centers, α_1 and α_2 are the scale factors of the length units in the front image planes given in pixel/m (Kelly, 1996; Adachi and Sato, 2004), R(ψ) and R(φ) are the rotation

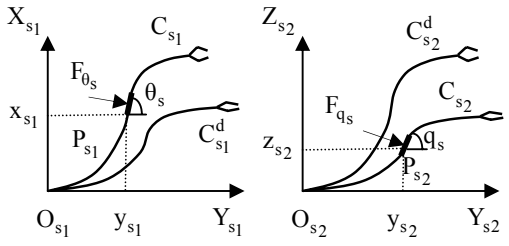

Fig. 4.

matrices generated by clockwise rotating the cameras about their optical axes by ψ and φ radians, respectively, and $[o_{11}, o_{12}]^T$ and $[o_{21}, o_{22}]^T$ represent the distances between the optical axes and the XOY and ZOY planes, respectively. In Fig. 4 are presented the screen images of the two cameras. From the relations (3.4), (3.5), we obtain

$$\begin{bmatrix}\Delta x_{s_1}\\ \Delta y_{s_1}\end{bmatrix} = \alpha_1 \cdot \frac{\lambda_1}{\lambda_1 - (D_1 + x)} \cdot \begin{bmatrix}\Delta x\\ \Delta y\end{bmatrix} \qquad (3.6)$$

$$\begin{bmatrix}\Delta z_{s_2}\\ \Delta y_{s_2}\end{bmatrix} = \alpha_2 \cdot \frac{\lambda_2}{\lambda_2 - (D_2 + x)} \cdot \begin{bmatrix}\Delta z\\ \Delta y\end{bmatrix} \qquad (3.7)$$

and the orientation angles for each plane will be

$$tg\theta_s = \frac{\Delta x_{s_1}}{\Delta y_{s_1}} = \frac{\Delta x}{\Delta y} = tg\theta \qquad (3.8)$$

hence

$$\theta_s(s') = \theta(s) \qquad , s \in [0,l], s' \in [0,l'] \qquad (3.9)$$

for the plane $Z_{S_1} O_{S_1} Y_{S_1}$ and

$$tgq_s = \frac{\Delta z_{s_2}}{\Delta y_{s_2}} = \frac{\Delta z}{\Delta y}$$

This relation allows the computation of the orientation angle q_s in the plane $Z_{S_2} O_{S_2} Y_{S_2}$

$$tgq_s(s'') = tgq(s) \cdot \frac{1}{\cos\theta(s)} \qquad (3.10)$$

where, $s \in [0,l]$,, $s'' \in [0,l'']$ s', s'' and l', l'' represent the projections of the variable s and the length l in the two planes, respectively. The projection of the forces on the two planes can be easily inferred from the Fig. 2 and the relations (3.8)-(3.10),

$$F_{\theta_s} = F_\theta \qquad (3.11)$$

$$F_{q_s} = F_q \cdot \sqrt{\cos^2 q + \sin^2 q \cdot \cos^2 \theta} \qquad (3.12)$$

4. SERVOING SYSTEM

The control system is an image – based visual servo control where the error control signal is defined directly in terms of image feature parameters.

The desired position of the arm in the robot space is defined by the curve C^d,

$$C : (\theta^d(s), q^d(s)) \quad , s \in [o,l] \qquad (4.1)$$

or, in the two image coordinate frames $Z_{S_1} O_{S_1} Y_{S_1}$ and $Z_{S_2} O_{S_2} Y_{S_2}$, by the projection of the curve C,

$$C^d_{s_1} : (\theta^d_s(s')) \quad , s' \in [0,l'] \qquad (4.2)$$

$$C^d_{s_2} : (q^d_s(s'')), s'' \in [0,l''] \qquad (4.3)$$

Define the motion errors as

$$e_\theta(t,s) = \theta(t,s) - \theta_d(s) \, , s \in [0,l] \qquad (4.4)$$

$$e_q(t,s) = q(t,s) - q_d(s) \, , s \in [0,l] \qquad (4.5)$$

or, in the image coordinate frames, by

$$e_{\theta_s}(t,s') = \theta_s(t,s') - \theta^d_s(s') \, , s' \in [0,l'] \qquad (4.6)$$

$$e_{q_s}(t,s'') = q_s(t,s'') - q^d_s(s'') \, , s'' \in [0,l''] \qquad (4.7)$$

The global control system is presented in Fig. 5. The control problem of this system is a direct visual servocontrol but we do not use the clasical concept of the position control in which is minimized the error between the robot end-effector and target. In this paper we will use the control of the shape of the curve in each point of the mechanical structure. The method is based on the particular structure of the system defined as a "backbone with two continuous angles θ(s) and q(s)".

The control of the system is based on the control of the two angles θ(s) and q(s). These angles are measured directly or indirectly. The angle θ(s) is measured dircetly by the projection on the image plane $Z_{S_1} O_{S_1} Y_{S_1}$ (relation 3.9) and q(s) is computed from the projection on the image plane $Z_{S_2} O_{S_2} Y_{S_2}$ (relation 3.10).

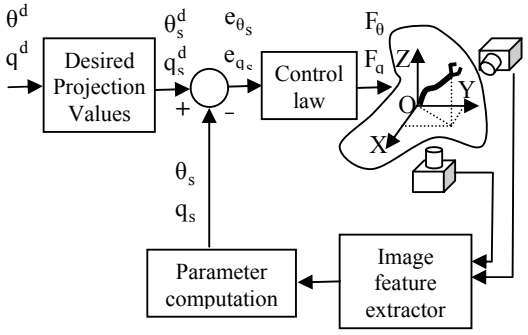

Fig. 5.

The stability of the closed-loop system is proven by the Lyapunov's second method but, in order to avoid the complex problems derived by using the nonlinear derivation integral model, in this paper will be developed a method based on the energy-work relationship (Wang et al., 2001).

Propostion The closed-loop hyperredundant arm system is stable if the control law is given by

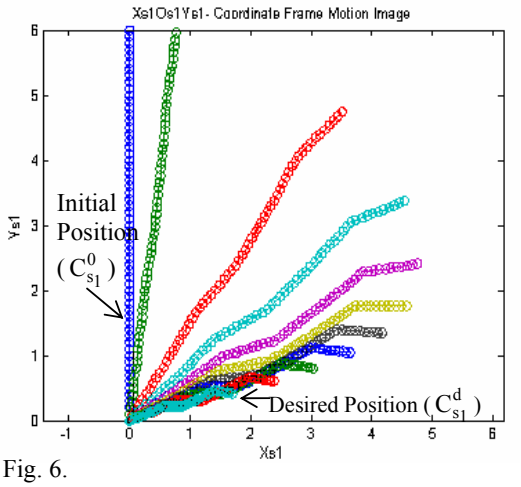

Fig. 6.

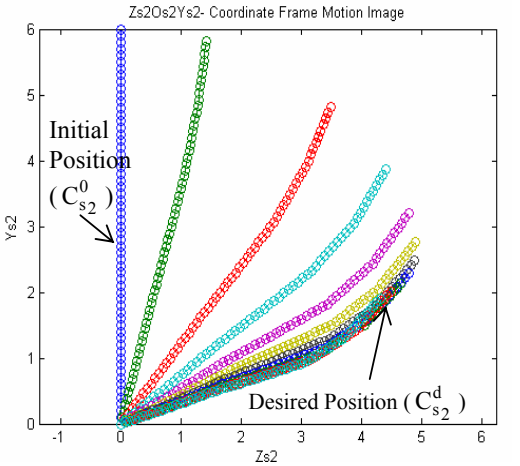

Fig. 7.

$$F_\theta(s,t) = -k_\theta^1(s)\cdot e_{\theta_s}(s',t) - k_\theta^2(s)\cdot \dot{e}_{\theta_s}(s',t) \quad (4.8)$$

$$F_q(s,t) = -k_q^1(s)\cdot\left[tg^{-1}(\cos\theta_s(s',t))\cdot \cdot \mathrm{tgq_s}(s'',t) - \mathrm{q^d}(s)\right] \quad (4.9)$$

where $s'\in[0,l']$, $s''\in[0,l'']$ and $k_\theta^1(s), k_\theta^2(s), k_q^1(s)$ are positive coefficients of the control law for all $s\in[0,l]$. The parameter of the control law (4.8), (4.9), can be inferred from the image feature extraction of the two planes. The parameters e_{θ_s} can be directly calculated from equation 4.6 and $\dot{e}_{\theta_s}$ can be indirectly computed. Also θ_s , q_s and q_s^d are evaluated directly from the trajectory projections. We remark that the control law (4.8), (4.9) represents a robust control, independent of the camera parameters. No intrinsec camera parameters are assumed to be known.

5. SIMULATION

Consider a hyperredundant manipulator that operates in OXYZ space. For simulation the following

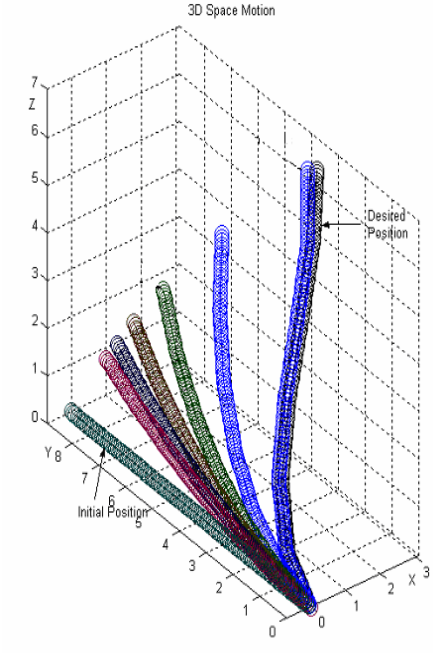

Fig. 8.

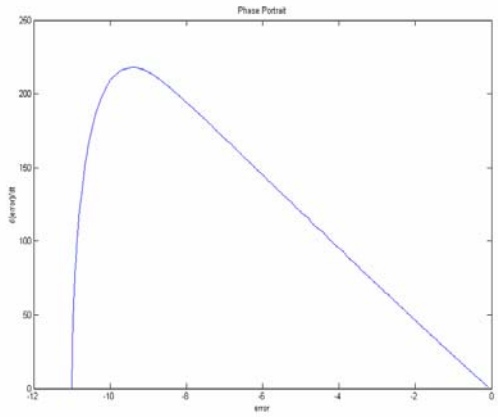

Fig. 9.

parameters will be assumed: the linear density $\rho = 2.2$ kg/m and the length $l = 0.6$ m. The integral differential model (A.1.9), (A.1.10) is simulated by using a discretization of the length with an increment $\Delta = 0.1$ m and a discret spatial s will be $s_i = i\cdot s$, i=1,2..6. The MATLAB Simulink is used. The initial position of the arm is assumed to be on the OY-axis and it is defined by the two image curves,

$$C_{s_1}^0 : \quad \theta_s^0(s_i') = 0 \ ,\mathrm{i}=1,2..6 \quad (5.1)$$

$$C_{s_2}^0 : \quad q_s^0(s_i'') = 0 \ ,\mathrm{i}=1,2..6 \quad (5.2)$$

The desired position is defined by the curves:

$$C_{s_1}^d : \quad \{ \quad \theta_s^d(s_1') = \pi/6; \theta_s^d(s_2') = \pi/8; \theta_s^d(s_3') = \pi/10;$$
$$\theta_s^d(s_4') = \pi/8; \theta_s^d(s_5') = \pi/6; \theta_s^d(s_6') = \pi/4; \quad \} \quad (5.3)$$

$$C^d_{s_2}: \quad \{ \quad q^d_s(s''_1)=\pi/6; q^d_s(s''_2)=\pi/8; q^d_s(s''_3)=\pi/10; \quad q^d_s(s''_4)=\pi/12; q^d_s(s''_5)=\pi/16; q^d_s(s''_6)=-\pi/24; \quad \} \quad (5.4)$$

The control laws (4.8), (4.9) is applied when the proportional and derivative coefficients are related as

$$k^1_\theta(s)=k^1_q(s)=173.6; k^2_\theta(s)=5.6 \quad (5.5)$$

The evolution of the arm is shown in the image planes $X_{S_1}O_{S_1}Y_{S_1}$, $Z_{S_2}O_{S_2}Y_{S_2}$ (Fig. 6 and Fig.7). We remark the motion of the arm projections to the desired position by several iteration positions. By using the relations (3.9), (3.10) the angles θ and q in 3D space are computed and the spatial arm is plotted in Fig.8. The quality of the control system can be appreciated by using the phase portrait of the evolution. The 3D error of the motion is defined by

$$e(t)=\int_0^1 \left(\left(q(s,t)-q_d(s)\right)-\left(\theta(s,t)-\theta_d(s)\right)\right)\cdot ds \quad (5.6)$$

The phase portrait is shown in Fig. 9. We remark the good stability of motion and the convergence to zero of the error.

6. CONCLUSIONS AND FUTURE WORK

In this paper the method of image-based servoing for a hyperredundant arm is studied. Servoing is based on binocular vision, a continuous measure of the arm parameters derrived from the real-time computation of the binocular optical flow over the two images, is compared with the desired position of the arm.

The control error function is built in 3D cartesian space by the visual information obtained by two cameras in two image planes. The two 2D errors obtained in the two image planes are determined by the two differences between the actual and desired continuous angle values that define the projections of the arm shape. The plane errors can be considered as the errors of the arm shape. These errors are used to calculate the spatial error and a control law is synthesized. For the closed-loop control system and a control law the stability is proven by using the Lyapunov second method. The error function is computed in the image spaces virtually and no calibration (camera parameters) is required allowing the synthesis of more robust control laws.

Future work will implement a spatial distribute observer to increase the control quality of the servoing system.

REFERENCES

Adachi, J., and J. Sato (2004), Uncalibrated Visual Servoing from Projectiove Reconstruction of Control Values, *Proceedings of the 17th International Conference on Pattern Recognition (ICPR '04)*, pp. 1051-4651/04.

Chirikjian, G. S. (1993). A General Numerical Method for Hyper-redundant Manipulator Inverse Kinematics, *Proc. 2000 IEEE Int. Conf. on Rob. and Automation*, Atlanta, pp. 107-112.

Chirikjian, G. S. and J.W. Burdick (1990). An Obstacle Avoidance Algorithm for Hyper-redundant Manipulators, *Proc. 2000 IEEE Int. Conf. on Robotics and Automation*, Cincinnati, Ohio, pp. 625-631.

Chirikjian, G. S. and J.W. Burdick (1992). Kinematically Optimal Hyper-redundant Manipulator Configurations, *Proc. 2000 IEEE Int. Conf. on Rob. and Aut.*, Nice, pp. 415-420.

Chirikjian, G. S. and J.W. Burdick (1995). Kinematically Optimal Hyper-redundant Manipulator Configurations, *IEEE Transaction Robotics and Automation*, **vol. 11**, no. 6, pp. 794-798.

Gravagne, I.A. and I.D. Walker (2000). On the Kinematics of Remotely – Actuated Continuum Robots, *Proc. 2000 IEEE Int. Conf. on Robotics and Automation*, San Francisco, pp. 2544-2550.

Grosso, E., G. Metta, A. Oddera and G. Sandrini (1996) Robust Visual Servoing in 3-D Reaching Tasks, *IEEE Trans. on Robotics and Automation*, **vol. 12**, Nr. 15, pp. 732-742.

Hemami, A. (1984). Design of Light Weight Flexible Robot Arm, *Robots 8 Conference Proceedings*, Detroit, USA, pp. 1623-1640.

Hutchinson, S., G.D. Hager and P.F. Corke (1996). A Tutorial on Visual Servor Control, *IEEE Trans. on Rob. and Aut.*, **vol. 12**, Nr. 15, pp. 651-670.

Ivanescu, M. (2002). Position Dynamic Control for a Tentacle Manipulator, *Proc. IEEE Int. Conf. on Rob. and Aut.* Washington, A1-15, 1531-1539.

Kelly, R. (1996). Robust Asymptotically State Visual Servoing of Planor Robots, *IEEE Trans. and Rob. and Aut.* **vol. 22**, Nr. 15, pp. 759-765.

Mochiyama, H. and H. Kobayashi (1999). The Shape Jacobian of a Manipulator with Hyper Degrees of Freedom, *Proc. 1999 IEEE Int. Conf. on Rob. and Automation*, Detroit, pp. 2837-2842.

Pressigout, M. and E. Marchand (2004), Model-free Augmented Reality by Virtual Visual Servoing, *Proceedings of the 17th International Conference on Pattern Recognition (ICPR '04)*, pp. 1051-4651/04.

Robinson, G. and J.B.C. Davies (1999). Continuum Robots – a State of the Art, *Proc. 1999 IEEE Int. Conf. on Robotics and Automation*, Detroit, Michigan, pp. 2849-2854.

Wang, P. K. C. (1965). Control of Distributed Parameter Systems, *Advance in Control Systems*, by C. T. Leondes, Academic Press.

Wang, Z. P., S.S. Ge and T.H. Lee (2001). Non-Model-Based Robust Control of Multi-Link Smart Material Robots, *Asian Conference on Rob. and Its App.*, Singapore, pp. 268-273.